Supplemental Document

Biomedical Optics EXPRESS

In vivo fluorescence molecular imaging of the vascular endothelial growth factor in rats with early diabetic retinopathy: supplement

LU ZHANG,[1,2,3,7] YUNHE DING,[1,2,3,7] XINJIAN CHEN,[4,7] DEHUI XIANG,[4] FEI SHI,[4] YANYUN CHEN,[5] SHENSHEN YAN,[5] XINYUAN ZHANG,[5] JIE TIAN,[3] SOBHA SIVAPRASAD,[6] YANG DU,[3,8] ZHI YANG,[1,2,9] AND BEI TIAN[5,10]

[1]*School of Biomedical Engineering, Capital Medical University, Beijing, 100069, China*
[2]*Beijing Key Laboratory of Fundamental Research on Biomechanics in Clinical Application, Capital Medical University, Beijing, 100069, China*
[3]*CAS Key Laboratory of Molecular Imaging, The State Key Laboratory of Management and Control for Complex Systems, Institute of Automation, Chinese Academy of Sciences, Beijing, 100190, China*
[4]*School of Electronics and Information Engineering and the State Key Laboratory of Radiation Medicine and Protection, Soochow University, Jiangsu, 215006, China*
[5]*Beijing Tongren Eye Center, Beijing Tongren Hospital, Capital Medical University, Beijing, 100730, China*
[6]*NIHR Moorfields Biomedical Research Centre, Moorfields Eye Hospital, London, EC1 V 2PD, UK*
[7]*These authors contributed equally to this work*
[8]*yang.du@ia.ac.cn*
[9]*zhiyang@ccmu.edu.cn*
[10]*tianbei@ccmu.edu.cn*

Supplement DOI: https://doi.org/10.6084/m9.figshare.16866301

Parent Article DOI: https://doi.org/10.1364/BOE.439446

In vivo fluorescence molecular imaging of vascular endothelial growth factor in rats with early diabetic retinopathy

Lu Zhang,[1, 2, 3, †] Yunhe Ding,[1,2, 3, †] Xinjian Chen,[4, †] Dehui Xiang,[4] Fei Shi,[4] Yanyun Chen, [5] Shenshen Yan,[5] Xinyuan Zhang,[5] Jie Tian,[3] Sobha Sivaprasad,[6] Yang Du,[3, 7] Zhi Yang,[1, 2, 8] and Bei Tian[5, 9]

[1]*School of Biomedical Engineering, Capital Medical University, Beijing, 100069, China*

[2]*Beijing Key Laboratory of Fundamental Research on Biomechanics in Clinical Application, Capital Medical University, Beijing, 100069, China*

[3]*CAS Key Laboratory of Molecular Imaging, The State Key Laboratory of Management and Control for Complex Systems, Institute of Automation, Chinese Academy of Sciences, Beijing, 100190, China*

[4]*School of Electronics and Information Engineering and the State Key Laboratory of Radiation Medicine and Protection, Soochow University, Jiangsu, 215006, China*

[5]*Beijing Tongren Eye Center, Beijing Tongren Hospital, Capital Medical University, Beijing, 100730, China*

[6]*NIHR Moorfields Biomedical Research Centre, Moorfields Eye Hospital, London, EC1V 2PD, United Kingdom*

[7] *yang.du@ia.ac.cn*

[8] *zhiyang@ccmu.edu.cn*

[9] *tianbei@ccmu.edu.cn*

[†] *These authors contributed equally to this work*

SUPPLEMENTARY FIGURES

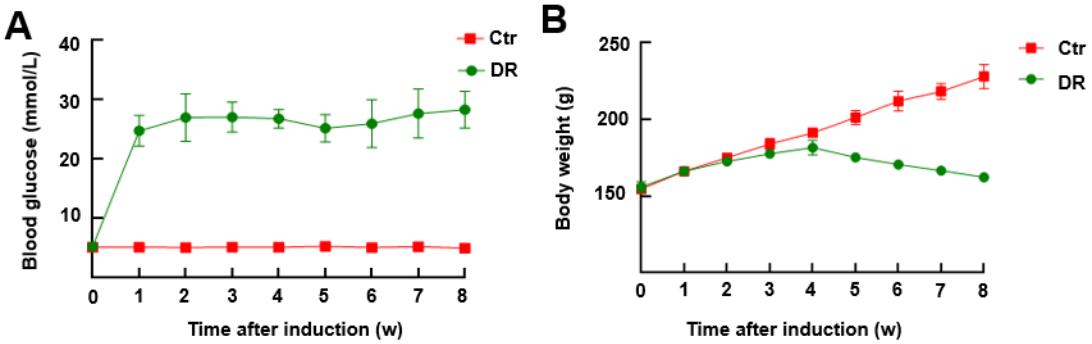

Fig. S1. Blood glucose levels and body weights of DR rat models over time after induction. (A) Blood glucose levels, and **(B)** Body weights of the animals used in the present study. Compared with the normal control group, the blood glucose in the model group was significantly higher than that in the control group, the body weight decreased markedly since the fourth week.

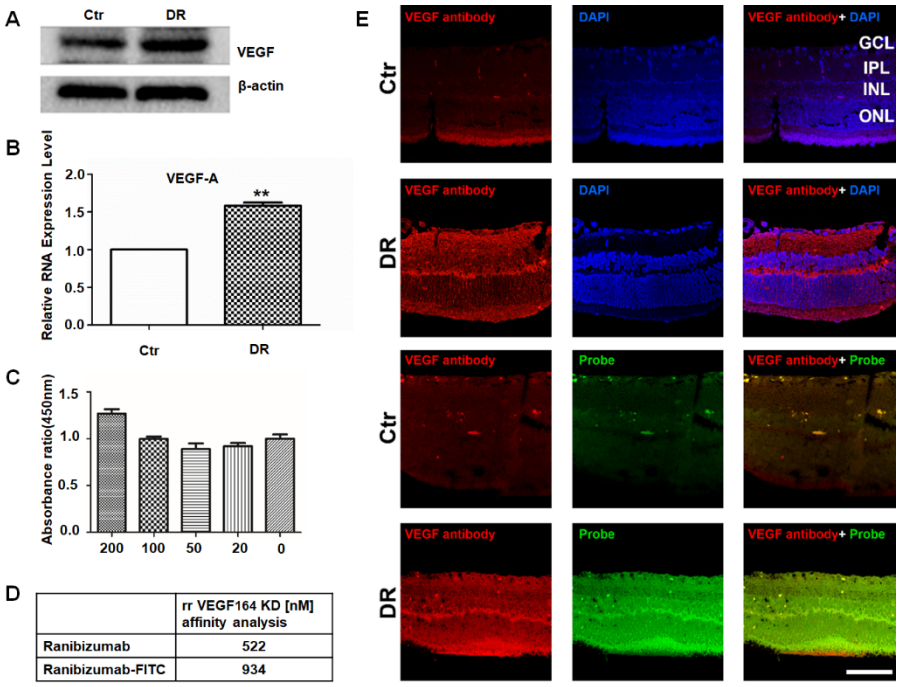

Fig. S2. The retinal VEGFA expression and the binding affinity tests. **(A)** Western blot analyses of VEGF-A in the retinas of normal and DR rats. VEGF expression was significantly increased in DR rats (n = 8 eyes, two rats per group). **(B)** qRT-PCR analyses of VEGF-A mRNA in the retinas of normal and DR rats. VEGF expression was also significantly increased in DR rats (n = 8 eyes, two rats per group). **(C)** *In vitro* studies revealed no toxic effects of the fluorescence probe with respect to the viability of human umbilical vein endothelial cells (HUVECs). Cell proliferation of HUVECs, as monitored by the Cell Counting Kit-8 assay, was enhanced by vascular endothelial growth factor (VEGF) in a dose dependent manner and ranibizumab inhibited this effect. **(D)** The binding affinity of ranibizumab and ranibizumab-FITC **(E)** Representative images of immunofluorescence of VEGF in the retina from paraffin sections. While low VEGF was detected in normal rats (first row), more robust VEGF signals in the GCL, IPL, and INL were found with the traditional immunofluorescence method in DR retina slices (second row). The double staining of VEGF antibody and fluoresce probe were shown in the third and fourth rows. Excellent VEGF colocalization was demonstrated by the VEGF antibody and the fluorescence probe. It indicated the fluorescence probe's VEGF binding and targeting ability. (n = 9 slices from 3 rats per group, bar= 75 μm). GCL: ganglion cell layer; IPL: inner plexiform layer; INL: inner nuclear layer; ONL: outer plexiform layer; Ctr, control.

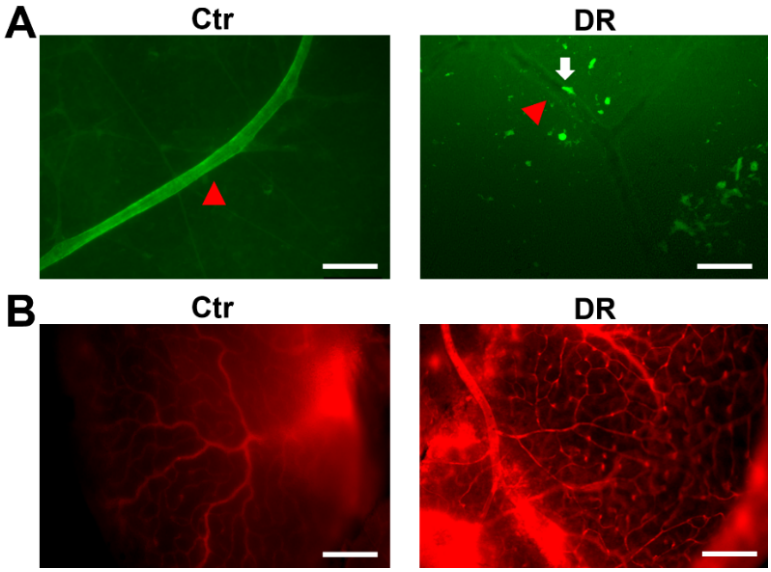

Fig. S3. ***Ex vivo*** **retinal flatmount fluorescent images of normal and diabetic retinopathy (DR) rats under an inverted fluorescence microscope. (A)** Images of the VEGF fluorescent probe. In the control group (left), the vascular structure was clear, and the probe was located inside the blood vessel. Due to the low level of VEGF in normal samples, the unbonded fluorescent probe entered into the venous system for metabolism. In the DR model (right), the fluorescent probes (white arrow) were scattered around the vessel wall (red arrowheads). Seventy-two hours following injection, only stationary bonded fluorescent probes could be seen in the image, indicating VEGF distribution (bar = 200 μm). **(B)** Blood vessels stained with Evans blue (EB). There were no vascular abnormalities in the control group (left). In the DR model (right), there are a large number of dilated capillary broken ends, neovascular buds, and hyper fluorescence outside the vessels, suggesting extensive destruction of the capillary bed and retinal venule leakage (bar = 100 μm). Ctr, control; DR, Diabetic retinopathy.

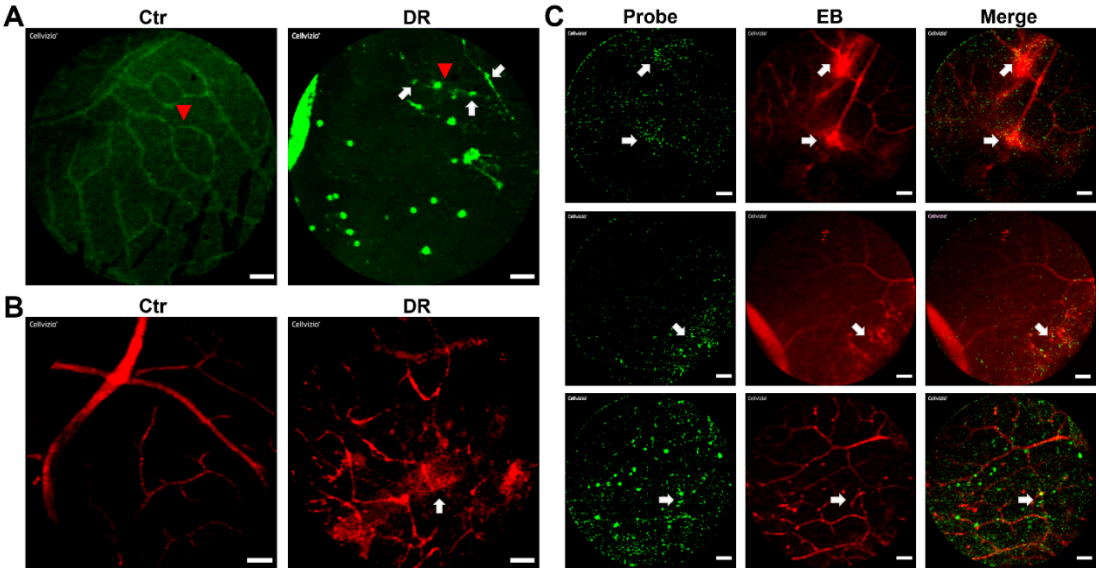

Fig. S4. ***Ex vivo*** **retinal flatmount fluorescent images of normal and diabetic retinopathy (DR) rats under Cellvizio imaging. (A)** Images of the fluorescent probes. In the control group (left), the vascular structure was clear and the probes were located inside the blood vessel (red arrowhead). Due to the low level of VEGF in normal samples, the unbonded fluorescent probe entered into the venous system for metabolism. In the DR model (right), the fluorescent probes (white arrow) were scattered around the vessel wall (red arrowheads). Seventy-two hours following injection, only stationary bonded fluorescent probes could be seen in the image, indicating VEGF distribution. **(B)** Blood vessels stained with Evans blue (EB). In the control group, no vascular abnormalities were found. In the DR model, the blood vessels stained with EB are intermittent. Some dye diffusion (white arrow) was observed, indicating leakage of blood vessels caused by the high expression of VEGF and the apoptosis of perivascular cells. **(C)** Colocalization of fluorescent probes and DR vascular lesions (white arrows), implying high VEGF expression, which may lead to this vascular damage (bar =50 μm). Ctr, control; DR, Diabetic retinopathy.

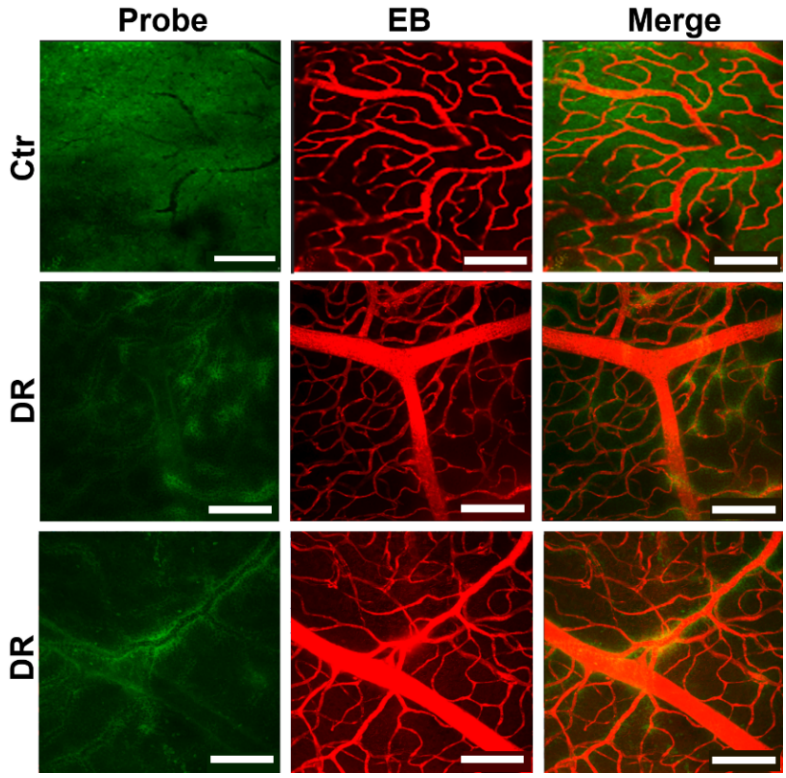

Fig. S5. ***Ex vivo*** **retinal flatmount images of normal and diabetic retinopathy (DR) rats under a confocal microscope.** In the control group, little positive fluorescence signal was observed by the VEGF probe. The blood vessels stained by Evans blue had smooth walls and regular bifurcations. In the DR model, the probes were mainly distributed around the vessels, especially at the bifurcations, which indicated that the vascular lesions of DR caused by VEGF over expression may start from the vascular bifurcation (bar = 100 μm). (Ctr, control; DR, Diabetic retinopathy).

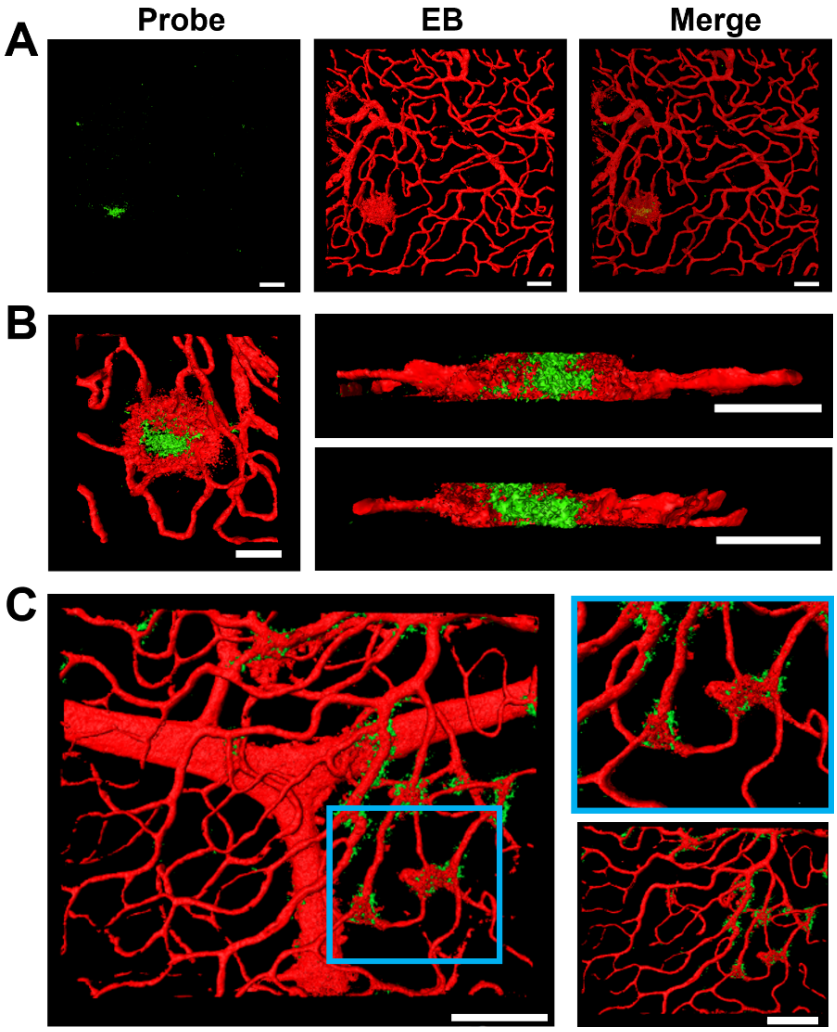

Fig. S6. **The binding characterization of VEGF to the vascular abnormities in diabetic retinopathy (DR) retinas. (A)** Three-dimensional (3D) surface rendering of blood vessels and probes. There was obvious aggregation of fluorescence probes in the microangioma. The right image is a transparent view of the vessels to demonstrate the anatomical relationship of the probe and the microangioma. Multiple small microangiomas fused to form a large microangioma, forming the early signs of intraretinal microvascular abnormality. Through the longitudinal section of two directions, it can be seen that massive amounts of fluorescent probes accumulated inside the hemangioma (bar = 30 μm). **(B)** Enlarged view of the hemangioma and two longitudinal sections of the 3D model. The enlarged image of the microangioma revealed that probes were aggregated and bound inside the vessel abnormality, indicating high VEGF expression (bar = 30 μm). **(C)** 3D view of the lesion area with the probe attached to the surface of the vessel (bar = 50 μm).